Article

Preparation and Characterization of Glucose-Based Self-Blowing Non-Isocyanate Polyurethane (NIPU) Foams with Different Acid Catalysts

Tianjiao Yang [1], Antonio Pizzi [2],*, Xuedong Xi [1], Xiaojian Zhou [1] and Qianyu Zhang [1],*

[1] Yunnan Key Laboratory of Wood Adhesives and Glued Products, College of Material Science and Chemistry Engineering, Southwest Forestry University, Kunming 650224, China; 15288047261@163.com (T.Y.); xuedong.xi@swfu.edu.cn (X.X.); xiaojianzhou@hotmail.com (X.Z.)

[2] LERMAB, University of Lorraine, 27 Rue Philippe Seguin, 88000 Epinal, France

* Correspondence: antonio.pizzi@univ-lorraine.fr (A.P.); zqy20160922@163.com (Q.Z.)

Abstract: The preparation and application of non-isocyanate polyurethane (NIPU) from biomass raw materials as a substitute for traditional polyurethane (PU) has recently become a research hot topic as it avoids the toxicity and moisture sensitivity of isocyanate-based PU. In the work presented here, self-blowing GNIPU non-isocyanate polyurethane (NIPU) rigid foams were prepared at room temperature, based on glucose, with acids as catalysts and glutaraldehyde as a cross-linker. The effects of different acids and glutaraldehyde addition on foam morphology and properties were investigated. The water absorption, compressive resistance, fire resistance, and limiting oxygen index (LOI) were tested to evaluate the relevant properties of the foams, and scanning electron microscopy (SEM) was used to observe the foams' cell structure. The results show that all these foams have a similar apparent density, while their 24 h water absorption is different. The foam prepared with phosphoric acid as a catalyst presented a better compressive strength compared to the other types prepared with different catalysts when above 65% compression. It also presents the best fire resistance with an LOI value of 24.3% (great than 22%), indicating that it possesses a good level of flame retardancy. Thermogravimetric analysis also showed that phosphoric acid catalysis slightly improved the GNIPU foams' thermal stability. This is mainly due to the flame-retardant effect of the phosphate ion. In addition, scanning electron microscopy (SEM) results showed that all the GNIPU foams exhibited similar open-cell morphologies with the cell pore sizes mainly distributed in the 200–250 μm range.

Keywords: glucose-based NIPU; self-blowing; rigid foams; fire resistance; acid catalysts

1. Introduction

Polyurethane (PU) foams are prepared by the polymerization foaming of isocyanates and hydroxyl compounds. They have a wide utilization in walls, pipe insulation materials, and building sound insulation materials due to their excellent elasticity, flexibility, elongation, and compressive strength [1–4]. However, PU foams inevitably require the use of a toxic isocyanate during their preparation and thus are harmful to humans and the environment [5,6]. Therefore, trying to improve their preparation and performance is at present of topical interest.

Currently, biomass foams have become a research hotspot with the development of biomass materials [7–9]. Although many works have reported the use of biomass polyols to prepare biomass-based PU foams, the process still uses isocyanates [10–15]. Therefore, NIPU has been synthesized to eliminate the harm of isocyanates while satisfying the performance required for polyurethanes [16]. NIPU has safer and more stable characteristics than isocyanate-based PU, while NIPU can present better water absorption, chemical resistance, and penetration resistance. This renders replacing traditional PU feasible, and

works have shown that it can be used in coatings, crack-resistant composites, adhesives, and sealants [17–21].

In general, NIPUs were initially prepared by reacting a cyclic carbonate with a polyamine by stepwise addition polymerization. Unfortunately, this method has some drawbacks, such as high pressure [22,23], high temperature [24], catalysts [24], the rather too slow opening of the cyclic carbonate for the further reaction for adhesives, and certain defects in the technology of synthesizing the cyclic carbonate [25–27]. Another way has been reported to prepare NIPU: cyclic carbonates were obtained with dimethyl carbonate and polyhydroxyles, and this method has no catalyst and a low time cost [28–31].

More recently, tannin-based NIPU foams were successfully prepared [32–35]. Moreover, works on preparing NIPU based on monosaccharides and disaccharides exhibited a good performance, especially applied to wood adhesive [16,30]. The preparation of glucose-based NIPU foams also has been reported [25,26]. However, a drawback is their requirement of a 200 °C temperature for their setting and their poor fire resistance. Their fire resistance has been greatly improved by preparing NIPU foams starting from a mixture of saccharides and tannins [6]. The work presented here is focused on the preparation of rigid foams by adding acid catalysts and aldehyde hardeners for room-temperature preparation and on studying the effect of different acids as catalysts on GNIPU self-blowing rigid foams.

2. Materials and Methods

2.1. Materials

Glucose (AR), phosphoric acid (AR), and formic acid (AR) were obtained from Guangdong Guanghua Technology Co., Ltd. (Shantou, China); maleic acid (AR) and hexamethylenediamine (AR) were obtained from Sinopharm Chemical Reagent Co., Ltd. (Beijing, China); dimethyl carbonate (AR, 99%) and glutaraldehyde (AR, 50% water solution) were purchased from Shanghai Macklin Biochemical Technology Co., Ltd. (Shanghai, China); citric acid (AR) was obtained from Tianjin Fengchuan Chemical Reagent Technology Co., Ltd. (Tianjin, China).

2.2. Synthesis of the Glucose-Based Non-Isocyanate Polyurethane (GNIPU) [25]

In total, 90 g of distilled water, 120 g of glucose, and 108 g of dimethyl carbonate were mixed in a three-necked flask, and the temperature was increased to 70 °C, keeping the reaction for 2 h. After that, 104.4 g of hexamethylene diamine was added to the mixture and stirred; then, the temperature was raised to 90 °C for a 30 min reaction. Next, the resin was cooled to room temperature and discharged.

2.3. Preparation of GNIPU Foams

The GNIPU was mixed with an acid (formic acid, maleic acid, phosphoric acid, and citric acid) and glutaraldehyde for foaming at room temperature. The obtained foams were maintained at room temperature for 30 min; then, they were dried in an oven at 73 °C for 10 h.

2.4. Water Absorption (24 h) Test

To investigate the effect of different initiators on the water absorption of GNIPU foams, the samples were cut to a size of 2 cm × 2 cm × 2 cm for 24 h water absorption tests. First, the foam was dried in the oven to record the mass (m); then, it was completely immersed in water and taken out according to the specified time; the surface moisture was wiped, and then, it was weighed (m'). The calculation formula of water absorption is $\frac{m'-m}{m} \times 100\%$. Each sample was tested three times to find the average value.

2.5. Compression Test

The obtained GNIPU foams were cut into 2 cm × 2 cm × 2 cm samples and subjected to compression testing. The test was performed on a UTM5105 series electronic universal

testing machine (Shenzhen Sansi Zongheng Technology Co., Ltd., Shenzhen, China) in an ambient environment with a testing rate of 2 mm/min.

2.6. Ignition Test

Foam samples of 2 cm × 2 cm × 2 cm cut from the foams prepared were placed in the outer flame of an alcohol lamp until the sample charred and did not burn anymore, and the time to reach this state was measured.

2.7. Limiting Oxygen Index (LOI)

The limiting oxygen index (LOI) was measured using an FTT0077 oxygen index meter (GBH International, St. Albans, Great Britain). All samples were prepared to a specification size of 80 mm × 10 mm × 10 mm.

2.8. TG Analysis

The thermal stability of the foams was studied using TG 209 F3 Tarsus® (Netzsch, Selb, Germany). In total, 5–8 mg of dried powder was placed into a platinum dish, and the sample was heated to the desired temperature at a heating rate of 10 K/min in a nitrogen atmosphere in the temperature range of 30–800 °C.

2.9. Fourier Transform Infrared (FT-IR) Spectrometry

To confirm the presence of relevant structures, Fourier transform infrared (FT-IR) analysis was carried out using an iS50 infrared spectrometer (Nicolet, Minneapolis, MN, USA). A blank sample tablet of potassium bromide was prepared for the reference spectrum. A similar tablet was prepared by mixing potassium bromide with 5% w/w of the sample powders to be analyzed. The spectrum was obtained in transmission measurement by combining 32 scans with a resolution of 2.0 cm^{-1} in the 400–4000 cm^{-1} range.

2.10. Scanning Electron Microscopy (SEM)

To investigate the cell microstructure and morphology of foams prepared with different initiators, scanning electron microscopy VEGA3, (TESCAN China, Chengdu, China) was used with an acceleration voltage of 20 kV. The cell size distributions of all foams were calculated by averaging several tens of individual cells for each sample.

3. Results and Discussion

3.1. GNIPU Foam Reaction Mechanism Analysis

The GNIPU self-blowing foams (F1, F2, F3, F4, F5, and F6) were prepared by adding acids and aldehydes at an ambient temperature. The foam formulations are shown in Table 1, and the samples are shown in Figure 1. From its appearance, the foam prepared with formic acid as an initiator has large cells, and the appearance of the other foams is not much different. The main predictable prepolymers formed by multiple reactions eventually lead to the structural network in the foam, as shown in Figure 2. The whole foaming process can be divided into two main steps: First is the start of the initial formation of the network. Glutaraldehyde is used as a cross-linker and reacts with the amino groups on the glucose-based NIPU prepolymer to ensure that the foam stays in shape (reaction formula (2)). The second step is the foaming process itself. In this stage, the acid reacts with the amino groups to catalyze self-blowing at room temperature (reaction formula (1)). Actually, these two processes occur almost simultaneously leading to finished foam.
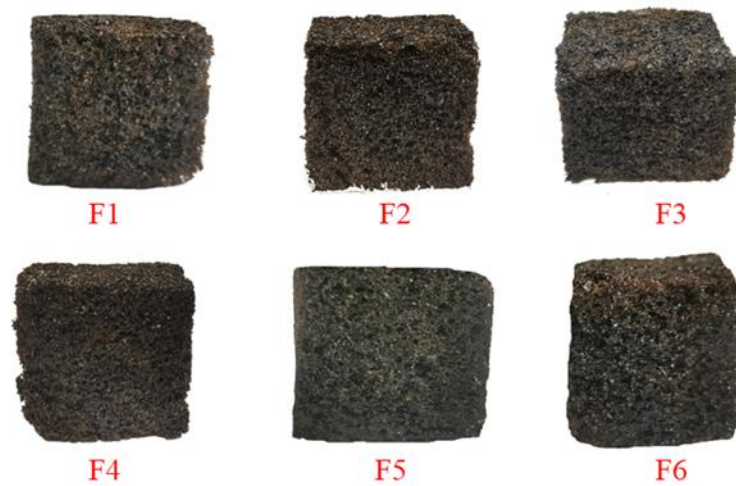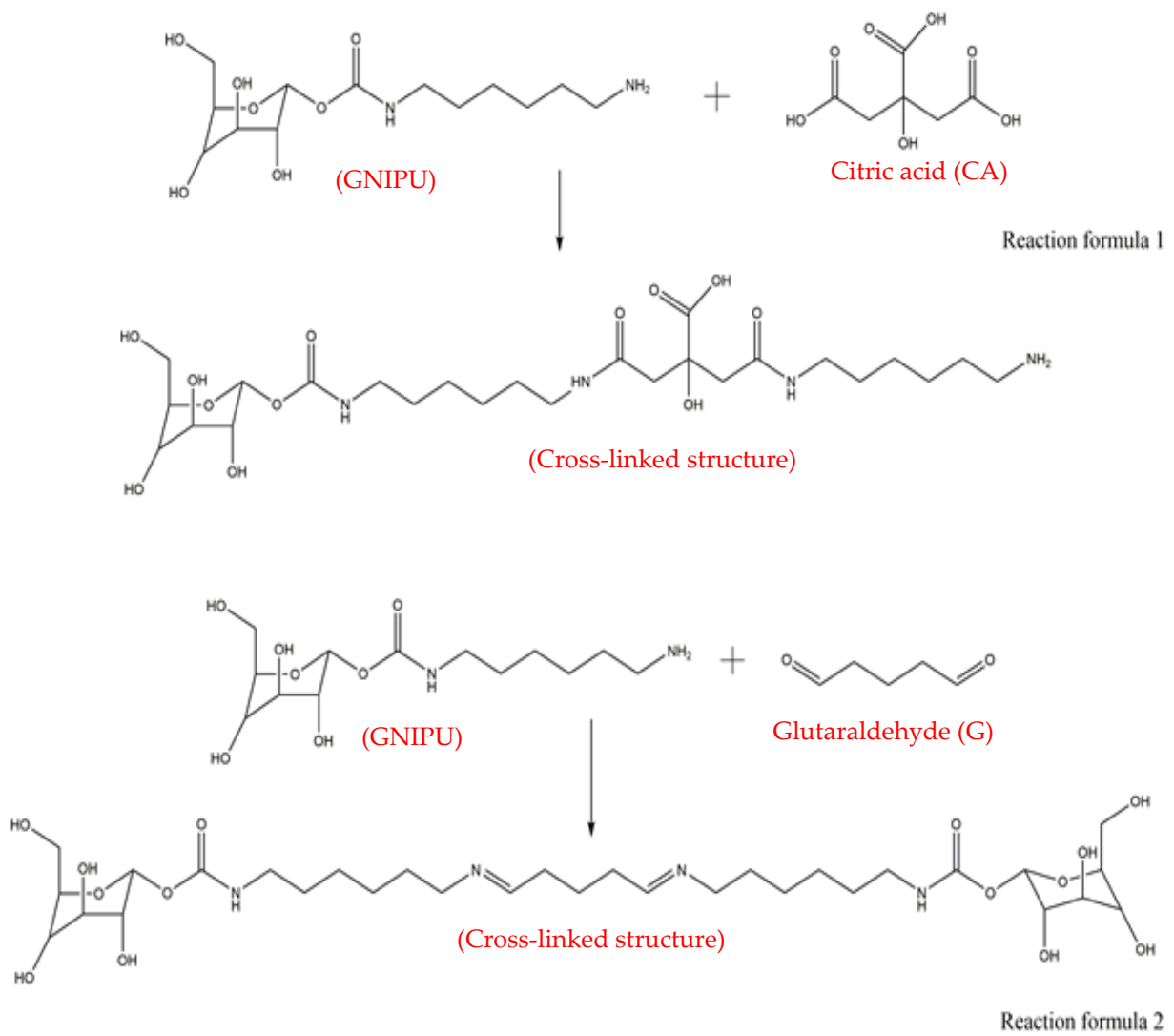
Figure 1. Photograph of GNIPU foams.

Figure 2. The main reactions leading to a cross-linked network in the foams.

Table 1. Performance of the GNIPU foams.

| Foam Number	Formulations	Density (g/cm³)	Ignition Time (s)
F1	10 g GNIPU + 1.0 g FA + 3.0 g G	0.119	75 s
F2	10 g GNIPU + 1.0 g MA + 3.0 g G	0.101	85 s
F3	10 g GNIPU + 1.0 g PA + 3.0 g G	0.105	0 s
F4	10 g GNIPU + 1.0 g CA + 3.0 g G	0.108	80 s
F5	10 g GNIPU + 1.0 g PA + 2.0 g G	0.107	0 s
F6	10 g GNIPU + 1.0 g PA + 4.0 g G	0.112	0 s

Note: FA—formic acid; MA—maleic acid; PA—phosphoric acid; CA—citric acid; G—glutaraldehyde.

3.2. Effects of Different Acid and Glutaraldehyde Additions on Basic Foam Properties

Regarding the performance of the GNIPU foams prepared with different catalysts, some of their tested results are shown in Table 1. By comparing foams F1, F2, F3, and F4, it appears that different catalysts do not seem to yield large differences in foam density and ignition time. The formic-acid-catalyzed foam density is only slightly higher than the others. The most likely explanation for this is a lesser catalyst acidity. Formic acid has the weakest acidity of the four acids tried; it reacts relatively gently with amino groups and thus cannot sufficiently catalyze the reaction. This means that mixtures of the same mass can only reach a smaller volume after foaming, thus presenting a higher density. By comparing foams F3, F5, and F6, it can be seen that the density and ignition time of the foams are not much affected by the amount of glutaraldehyde added.

3.3. Water Absorption of GNIPU Foams

Figures 3 and 4 show the 24 h water absorption of the GNIPU foams prepared according to the formulations in Table 1. First, the GNIPU foams in Figure 3 show different levels of water absorption, this being directly associated with their density and cell opening size. The foams showed a higher water absorption in the first 2.5 h. The water absorption tends to stabilize after about 2.5 h of water immersion due to a certain amount of water already being stored in the cell cavity and thus functioning as reverse hydrostatic pressure. The water absorption appears to be related to foam density, as the curves for lower density foams (F2, F3, and F4) grow slowly, while the denser foams (F1) increase rapidly. Figure 4 shows the same water absorption pattern, where the change in glutaraldehyde addition leads to a different water absorption rate. An increase in the amount of glutaraldehyde led to an improvement in the foam density and thus to a higher water absorption, which is consistent with the conclusion obtained from Figure 3.
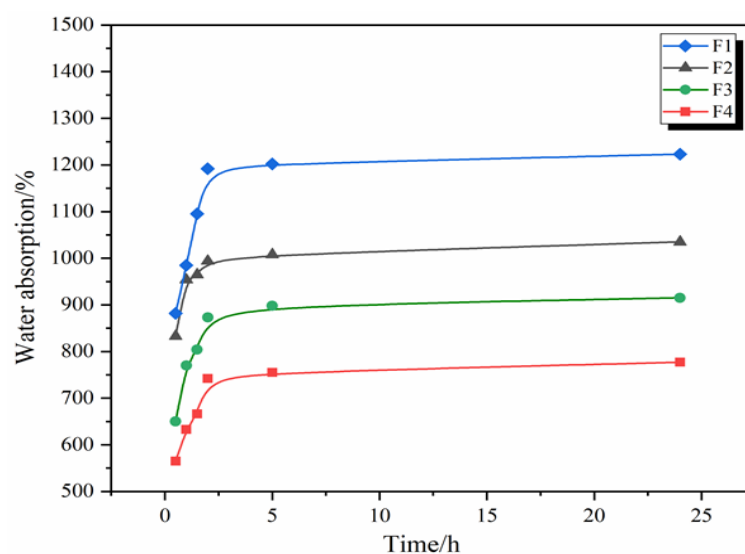
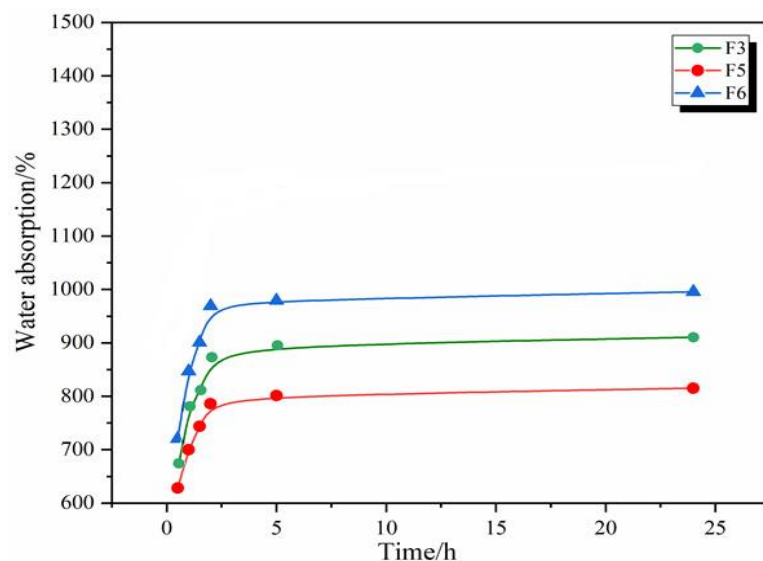**Figure 3.** Water absorption (24 h) of GNIPU foams (F1, F2, F3, and F4).

Figure 4. Water absorption (24 h) of GNIPU foams (F3, F5, and F6).

3.4. Compression Properties of GNIPU Foams

Figure 5 shows the compressive stress–strain curves of GNIPU foams F1, F2, F3, and F4 prepared with different acid catalysts. The stress of foam F1 is better than that of the other foams in the compression ratio of 0–65% range, this being due to its much higher density. The stress–strain curves of F2, F3, and F4 are similar in the 0–50% compression ratio range, due to their densities being similar. The reason for this is that the compression resistance is in direct relation to foam density [36]. Theoretically, fragile cell walls can only provide a limited contribution to compression resistance. The foam F1 was observed by scanning electron microscopy (SEM) to be more crumbly than the others, meaning that its cell walls are more brittle. Thus, the cell walls of foam F1 are more easily crushed at a high compression rate, so its stress–strain curves after a compression rate of 65% show a slower rate, with foam F3 showing a better compression resistance instead.
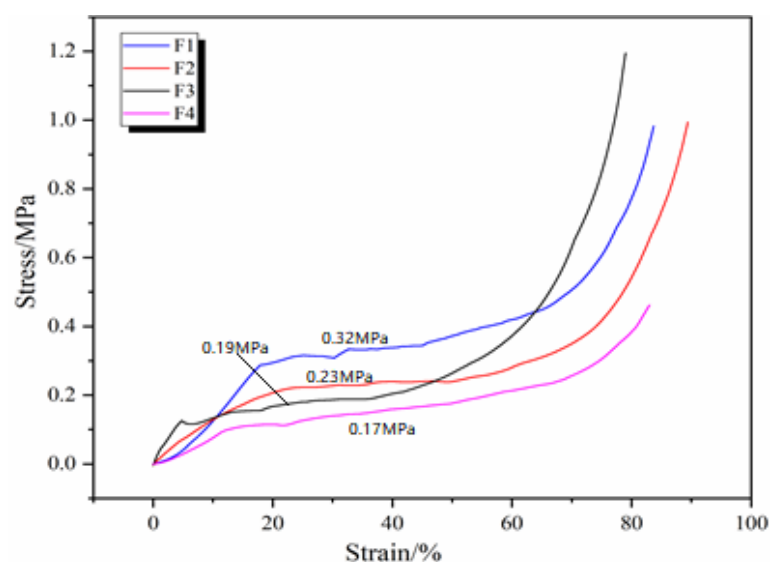

Figure 5. Effects of different initiators on compression performance of GNIPU foams.

Figure 6 shows the compressive stress–strain curves of GNIPU foams F3, F5, and F6 prepared with different additions of glutaraldehyde. It can be seen that at the same compression ratio, the more glutaraldehyde is added, the better the compressive properties are.

This is because the increase in the proportion of glutaraldehyde yields a more chemically cross-linked network, thus resulting in an improved resistance to compression.
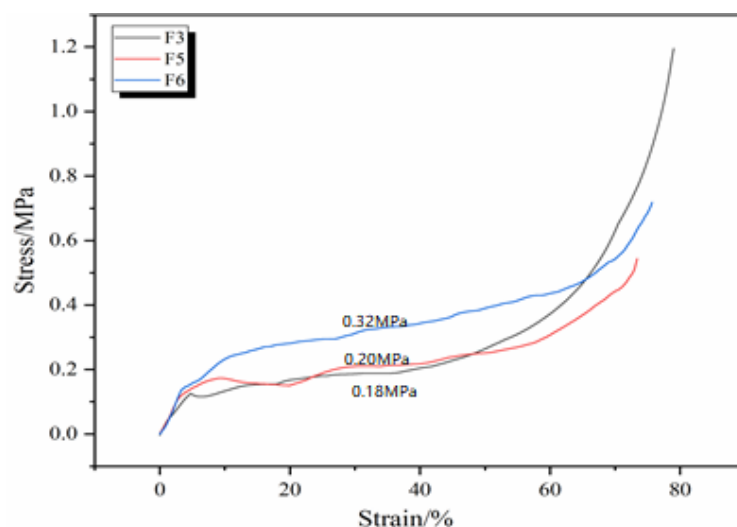

Figure 6. Effect of different additions of glutaraldehyde on compression properties of GNIPU foams.

3.5. Ignition Test Analysis

The ignition test results of the GNIPU foams are shown in Figure 7. The ignition test indicates to a certain extent the combustion resistance of the material, although with some clear limitations. Nonetheless, the fire resistance of the GNIPU foams prepared with different acid catalysts presents a clear certainty. The foams F1, F2, and F4 were flammable, and a very bright flame was observed in a very short time (10 s). At the same time, a large amount of black fumes (dotted red frame) were released when these foams were burned. Moreover, only completely irregular residues remained after foams F1, F2, and F4 were burned. This shows that these three foams are highly flammable, similarly to isocyanate-based PUs. However, the foams F3, F5, and F6 looked unburned. Furthermore, during ignition, only white smoke appeared, due to water vapor emission, and no large amount of black smoke was released (dotted blue frame), and the samples of foams F3, F5, and F6 after combustion kept their original shape. These results indicate that foam flammability is significantly reduced when the foam is prepared with phosphoric acid as a catalyst. It is well known that phosphorus compounds have been used as flame retardants for traditional isocyanate-based polyurethane foams. This is due to phosphorus compounds creating a coating that forms a carbon film on the foam surface to isolate oxygen and inhibiting combustion [37–40].

3.6. Limiting Oxygen Index (LOI) Analysis

The flame retardancy of polymers can be effectively evaluated by the limiting oxygen index (LOI), which reflects the lowest oxygen concentration when the polymer burns in a mixed nitrogen atmosphere and oxygen [41]. The LOI test results for all foams are shown in Figure 8. Generally, a material is classified as flammable when its LOI value is below 22%, and when the LOI value is above 27%, the material can be classified as flame-retardant. As expected, the LOI values of foams F1, F2, and F4 were 20.75%, 21.34%, and 20.9%, respectively, indicating that these foams are flammable. Combined with the SEM images, it can be observed that the open cell size of the foams F1, F2, and F4 is not much different, resulting in a very small difference in the oxygen concentration inside the foams and thus similar LOI values. Therefore, they need the addition of a flame retardant if one wants to improve their flame retardancy. The foam F3 prepared using phosphoric acid presenting a good flame-retardant effect also presents an LOI value of 24.3%. The LOI values of foams F5 and F6 were 24.19 and 24.59, respectively. Thus, the proportion of glutaraldehyde added did not affect the LOI values much. The cause of this is that phosphate itself is commonly

used as a flame retardant. The LOI test results of all foams also support the ignition test conclusion. Therefore, phosphoric acid as an initiator can improve the flame retardancy of GNIPU foam.
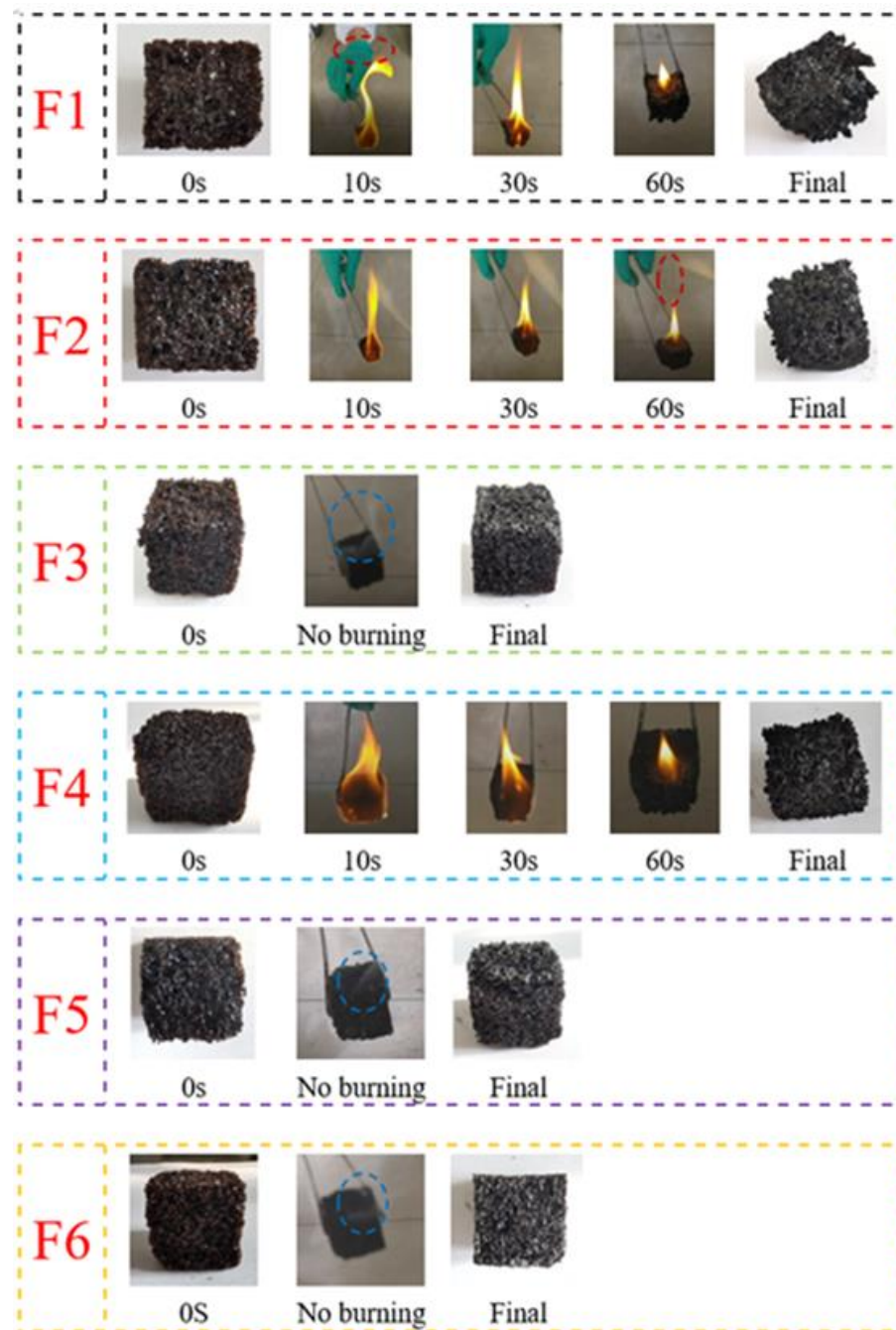
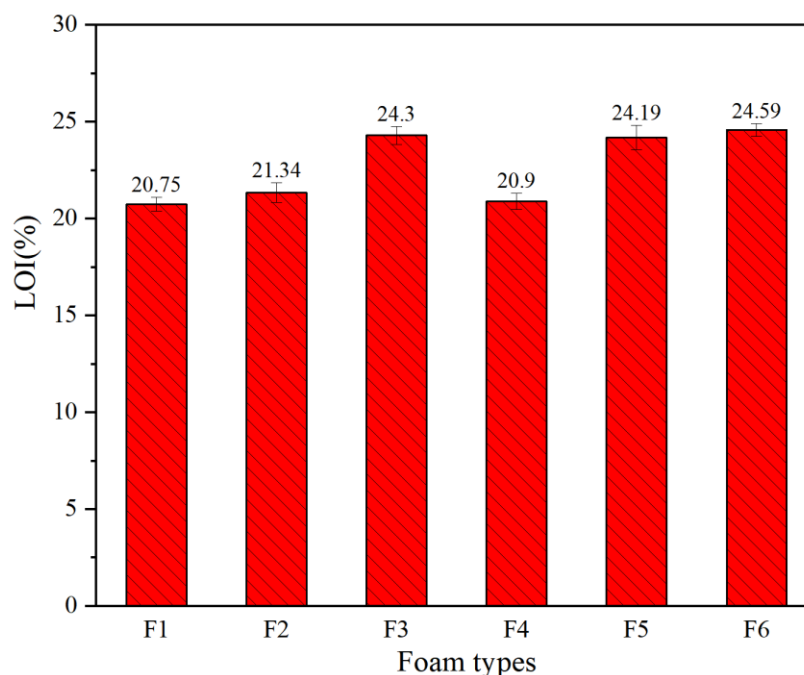

Figure 7. Photographic record of ignition experiments.

Figure 8. LOI of foams F1, F2, F3, F4, F5, and F6.

3.7. Thermogravimetric Analysis

Thermogravimetric analysis (TGA) was used to investigate the thermal stability of GNIPU foams. The TG (a) and DTG (b) curves of foams F1, F2, F3, and F4 under a N_2 atmosphere are shown in Figure 9. It can be noticed that the pyrolysis behavior of all foams was mainly divided into two decomposition stages. The first mass loss stage occurs in the temperature range of 30–280 °C, which belongs to the elimination and evaporation of impurities and water adsorbed on the surface of the solid foam powder. In addition, some small-molecule carbohydrate impurities and unstable chemical bonds were decomposed at this stage [27,42]. At the same time, an excess of hexamethylenediamine also leads to a quality loss at this stage due to the boiling point of hexamethylenediamine being around 200 °C. The second mass loss stage occurs between 300 °C and 600 °C and is mainly a mass loss stage. In this stage, the foam cross-linked network is progressively degraded and eventually destroyed [6].

In Figure 9, some obvious differences in pyrolysis behavior can be observed when the foam was prepared with different acid catalysts. The final residual mass percentage at 700 °C shows that these foams have a different mass loss percentage, the residual mass of foam F1 and F2 being around 11%, and foam F3 and F4 have the least mass loss with about 16% residual mass. In the second mass loss stage, F3 loses significantly less mass than F4. Furthermore, the decomposition temperature of foam F3 moves to a higher temperature than the others. These phenomena indicate that phosphoric acid catalysis increased the thermal stability of GNIPU foams, which is consistent with the ignition test and LOI results.
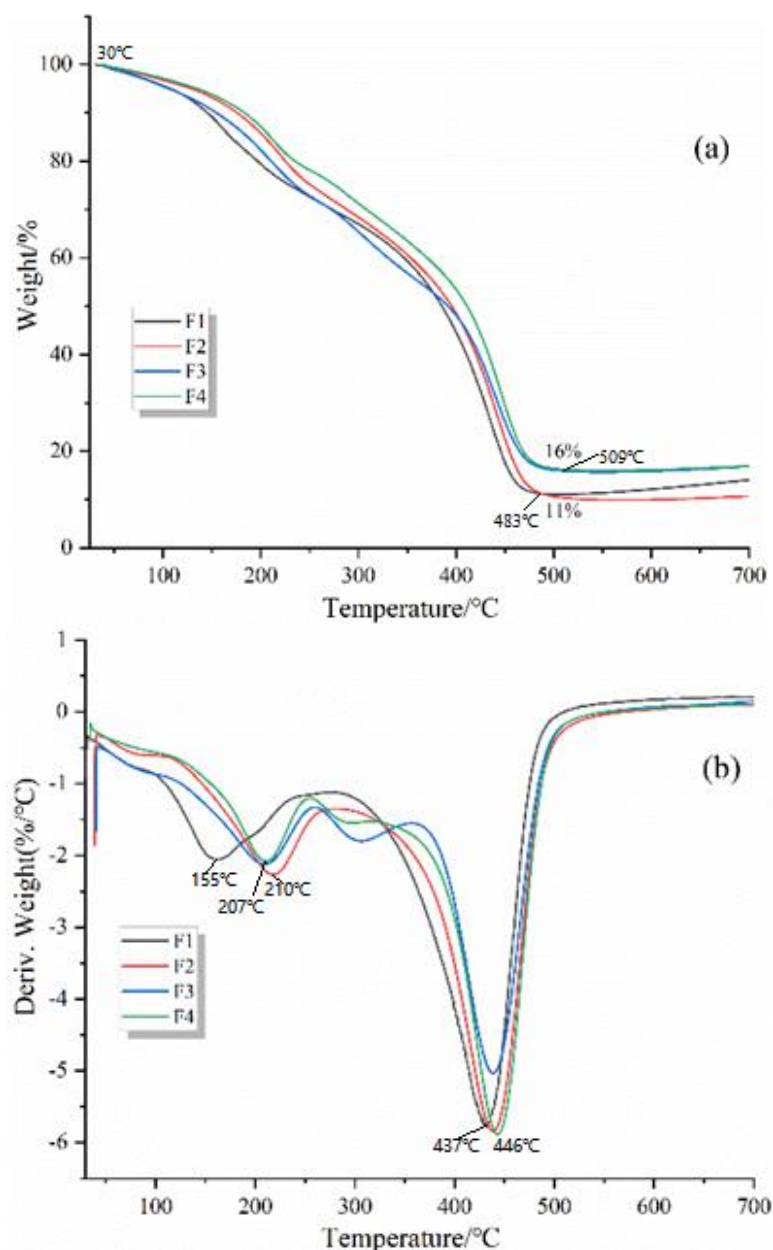
Figure 9. TG (**a**) and DTG (**b**) curves of GNIPU foams (F1, F2, F3, and F4).

3.8. Fourier Transform Infrared (FT-IR) Spectroscopy

The Fourier transform infrared (FT-IR) spectra of the GNIPU and all foams are shown in Figure 10. In Figure 10, a wide absorption peak at 3388 cm^{-1} is attributed to the O-H and N-H stretching vibration. The absorption peaks at 2930 cm^{-1} and 2857 cm^{-1} are attributed to the –CH$_2$– stretching vibration, which is related to the presence of HMDA [25,27]. Of these, the peaks at 1700 cm^{-1} and 1640 cm^{-1} are attributed to the C=O absorption of urethane groups and the N-H deformation of carbamate [43]. The urethane characteristic peak at 1548 cm^{-1} is related to C-N stretching [32,34]. In the FT-IR spectra of foams F1 and F4, the peaks at 1640 cm^{-1} are invisible due to the coincidence of the peaks of N-H and C-N. The absorption peak at 1254 cm^{-1} is characteristic of amino groups, which is decreased in F1, F2, F3, and F4 compared to GNIPU. This result is due to the acid and glutaraldehyde reaction with the amino groups in GNIPU.
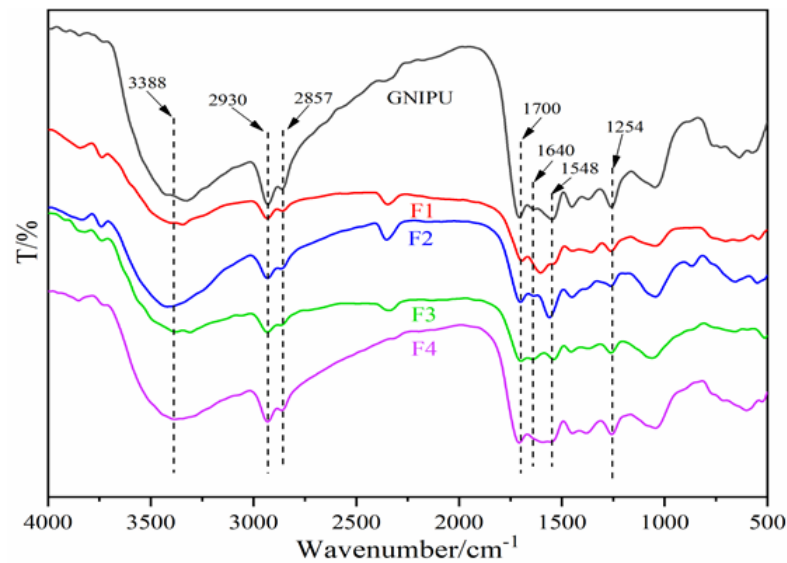
Figure 10. FT-IR spectra of GNIPU and foams (F1, F2, F3, and F4).

3.9. SEM Analysis

To explain the effects of the different catalysts on the F1, F2, F3, F4, F5, and F6 foam cell structures, these were observed by SEM and are shown in Figure 11. First, two different types of cells appear to be present in all foams, namely open and closed cells. It is easy to see that these foam structures mainly exist as open cells, which is caused by the evaporation of water in the resin during foaming and drying [6]. In addition, some rupture or debris, as well as incomplete cell structures, can be observed by SEM, this being due to the cutting process used to prepare the samples [41]. Second, by comparing different foams' SEM images, it appears that foam F1 has more debris due to its more brittle cell walls. The foam F3 has the thickest cell walls, explaining the best compression resistance in Figure 3. It is worth noting that foam F4 appears to have a more complete cell morphology, which is attributed to the citric acid catalyst that can also help to strengthen and stabilize the three-dimensional structure of the foam by a reaction with its constituents [44,45].
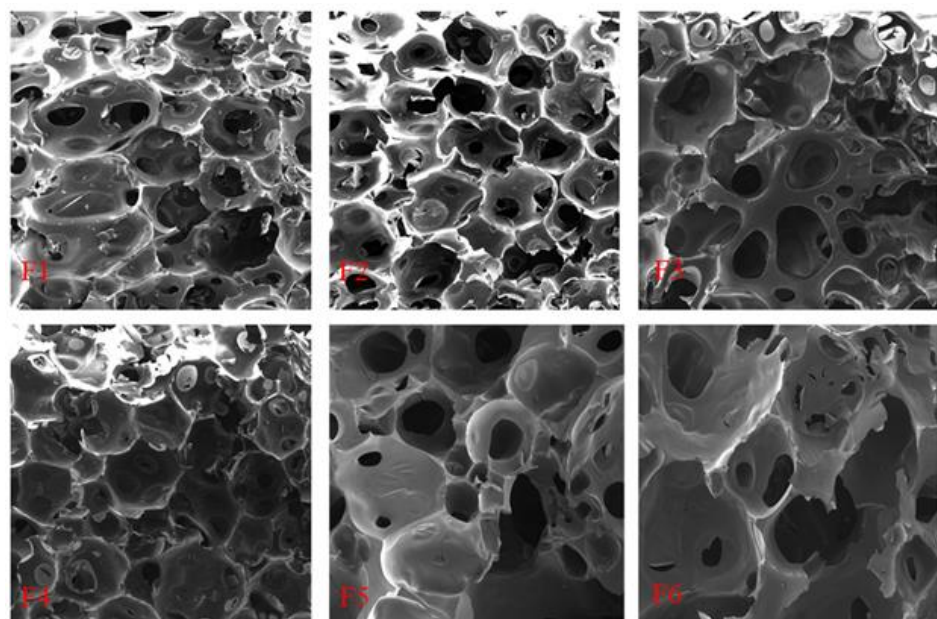

Figure 11. SEM pictures of GNIPU foams.

Figure 12 shows the results of the cell size distribution of GNIPU foams F1, F2, F3, F4, F5, and F6. It can be seen that the cell pore sizes of the four kinds of foam are mainly distributed in the 200–250 μm range. It can be noted that the cell pore size distribution of foam F4 prepared with citric acid is more concentrated. Furthermore, combining SEM pictures and Figure 12, the relationship of cell pore size is F2 > F6 > F3 > F5 > F4 > F1. In general, the foam pore size is inversely proportional to density. However, the cell pore sizes of the four foams are similar, also due to the fact that the density of the four foams is not much different.
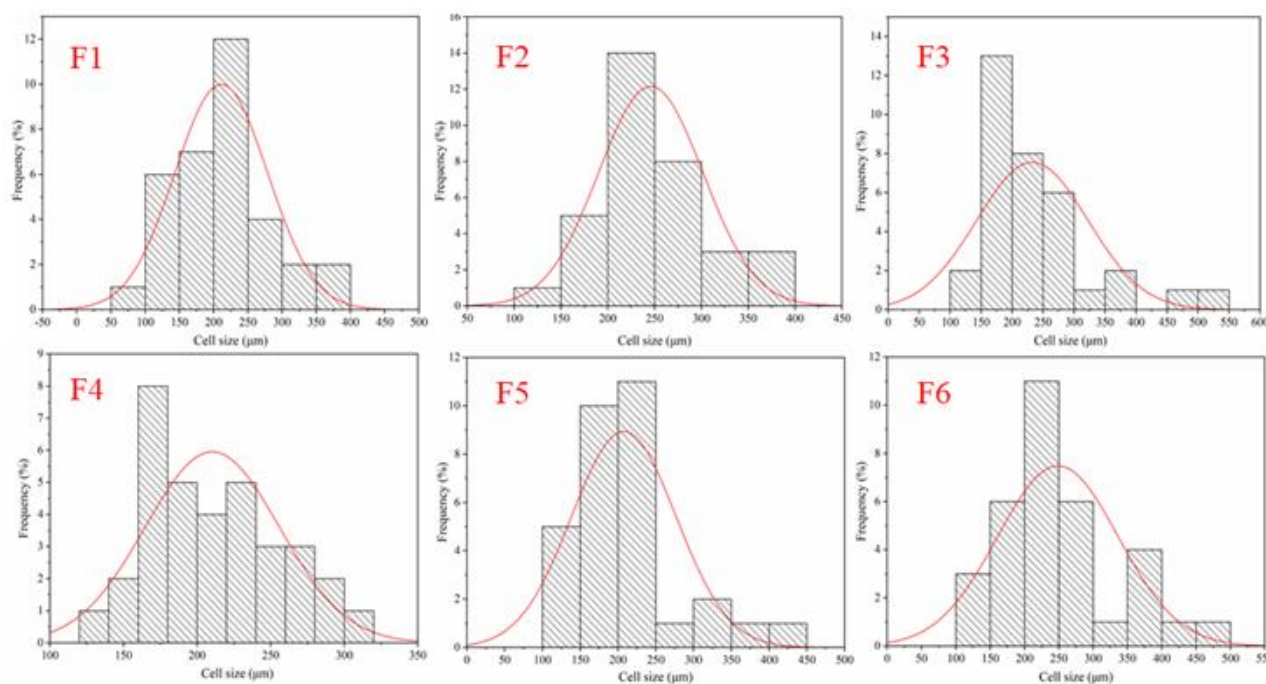

Figure 12. Cell size distributions of GNIPU foams. Gaussian cell size distribution curve indicated in red.

4. Conclusions

In this paper, the effects of different acids and glutaraldehyde addition on foam morphology and properties were investigated. The six kinds of foams exhibited a similar foam morphology and cell pore size. The compression mechanical properties are different owing to the different acid catalysts used. Foam F3 prepared with phosphoric acid had better compressive strength above 65% compression. The ignition test and limiting oxygen index test results indicated that the foams F1, F2, and F4 show high flammability, belonging to inflammable materials. However, the foam prepared with phosphoric acid has a certain flame retardancy. Simultaneously, foam F3 also shows better thermal stability. Some of these low-cost and non-toxic self-blowing GNIPU foams have a wide application potential, in particular the one prepared with phosphoric acid as a catalyst.

Institutional Review Board Statement: Not applicable.

Data Availability Statement: The original contributions presented in the study are included in the article, further inquiries can be directed to the corresponding authors.

Conflicts of Interest: The authors declare no conflicts of interest. The funders had no role in the design of this study; in the collection, analyses, or interpretation of data; in the writing of this manuscript; or in the decision to publish the results.

References

1. Gama, N.V.; Ferreira, A.; Barros-Timmons, A. Polyurethane foams: Past, present, and future. *Materials* **2018**, *11*, 1841. [CrossRef]
2. Kirpluks, M.; Kalnbund, D.; Benes, H.; Cabulis, U. Natural oil based highly functional polyols as feedstock for rigid polyurethane foam thermal insulation. *Ind. Crops Prod.* **2018**, *122*, 627–636. [CrossRef]
3. Gama, N.; Costa, L.C.; Amara, V.; Ferreira, A.; Barros-Timmons, A.M.M.V. Insights into the physical properties of biobased polyurethane/expanded graphite composite foams. *Comp. Sci. Technol.* **2017**, *138*, 24–31. [CrossRef]
4. Ji, Y.; Chen, S. Optimization of acoustic performances of a new tung oleic acid-based composite polyurethane foam. *J. Appl. Polym. Sci.* **2019**, *136*, 47861. [CrossRef]
5. Bourguignon, M.; Thomassin, J.M.; Grignard, B.; Jerome, C.; Detrembleur, C. Fast and facile one-pot one-step preparation of nonisocyanate polyurethane hydrogels in water at room temperature. *ACS Sustain. Chem. Eng.* **2019**, *7*, 12601–12610. [CrossRef]
6. Chen, X.; Li, J.; Xi, X.; Pizzi, A.; Zhou, X.; Fredon, E.; Du, G.; Gerardin, C. Condensed tannin-glucose-based NIPU bio-foams of improved fire retardancy. *Polym. Degrad. Stab.* **2020**, *175*, 109121. [CrossRef]
7. Tondi, G.; Zhao, W.; Pizzi, A.; Fierro, V.; Celzard, A. Tannin-based rigid foams: A survey of chemical and physical properties. *Bioresour. Technol.* **2009**, *100*, 5162–5169. [CrossRef]
8. Li, X.; Pizzi, A.; Cangemi, M.; Navarrete, P.; Segovia, C.; Fierro, V.; Celzard, A. Flexible natural tannin-based and protein-based biosourced foams. *Ind. Crops Prod.* **2012**, *37*, 389–393. [CrossRef]
9. Basso, M.C.; Pizzi, A.; Al-Marzouki, F.; Abdalla, S. Horticultural/hydroponics and floral natural foams from tannins. *Ind. Crops Prod.* **2016**, *87*, 177–181. [CrossRef]
10. Zhang, J.; Hori, N.; Takemura, A. Optimization of agricultural wastes liquefaction process and preparing bio-based polyurethane foams by the obtained polyols. *Ind. Crops Prod.* **2019**, *138*, 111455. [CrossRef]
11. Li, H.; Xu, C.C.; Yuan, Z.; Wei, Q. Synthesis of bio-based polyurethane foams with liquefied wheat straw: Process optimization. *Biomass Bioenergy* **2018**, *111*, 134–140. [CrossRef]
12. Yan, Y.; Pan, H.; Yang, X.; Zhang, R.; Liao, B. Preparation and characterization of water-blown polyurethane foams from liquefied cornstalk polyol. *J. Appl. Polym. Sci.* **2008**, *110*, 1099–1111. [CrossRef]
13. Li, H.; Feng, S.; Yuan, Z.; Wei, Q.; Xu, C.C. Highly efficient liquefaction of wheat straw for the production of bio-polyols and bio-based polyurethane foams. *Ind. Crops Prod.* **2017**, *109*, 426–433. [CrossRef]
14. Hu, S.; Wan, C.; Li, Y. Production and characterization of biopolyols and polyurethane foams from crude glycerol based liquefaction of soybean straw. *Bioresour. Technol.* **2012**, *103*, 227–233. [CrossRef]
15. Gómez-Fernández, S.; Günther, M.; Schartel, B.; Corcuera, M.A.; Eceiza, A. Impact of the combined use of layered double hydroxides, lignin and phosphorous polyol on the fire behavior of flexible polyurethane foams. *Ind. Crops Prod.* **2018**, *125*, 346–359. [CrossRef]
16. Xi, X.; Wu, Z.; Pizzi, A.; Geradin, C.; Lei, H.; Zhang, B.; Du, G. Non-isocyanate polyurethane adhesive from sucrose used for particleboard. *Wood Sci. Technol.* **2019**, *53*, 393–405. [CrossRef]
17. Figovsky, O.; Shapovalov, L.; Buslov, F. Ultraviolet and thermostable non-isocyanate polyurethane coatings. *Surf. Coat. Intern. Part B Coat. Trans.* **2005**, *88*, 67–71. [CrossRef]
18. Asemani, H.R.; Mannari, V. Synthesis and evaluation of non-isocyanate polyurethane polyols for heat-cured thermoset coatings. *Prog. Org. Coat.* **2019**, *131*, 247–258. [CrossRef]
19. Wu, Z.; Tang, L.; Dai, J.; Qu, J. Synthesis and properties of fluorinated non-isocyanate polyurethanes coatings with good hydrophobic and oleophobic properties. *J. Coat. Technol. Res.* **2019**, *16*, 1233–1241. [CrossRef]
20. Sarazin, J.; Pizzi, A.; Amirou, S.; Schmidt, D.; Sernek, M. Organosolv lignin for non-isocyanate based polyurethanes (NIPU) as wood adhesive. *J. Renew. Mater.* **2021**, *9*, 881–907. [CrossRef]
21. Poussard, L.; Mariage, J.; Grignard, B.; Detrembleur, C.; Jérôme, C.; Calberg, C.; Heinrichs, B.; De Winter, J.; Gerbaux, P.; Raquez, J.-M.; et al. Non-isocyanate polyurethanes from carbonated soybean oil using monomeric or oligomeric diamines to achieve thermosets or thermoplastics. *Macromolecules* **2016**, *49*, 2162–2171. [CrossRef]
22. Lee, A.; Deng, Y. Green polyurethane from lignin and soybean oil through non-isocyanate reactions. *Eur. Polym. J.* **2015**, *63*, 67–73. [CrossRef]

23. Esmaeili, N.; Vafayan, M.; Salimi, A.; Zohuriaan-Mehr, M.J. Kinetics of curing and thermo-degradation, antioxidizing activity, and cell viability of a tannic acid based epoxy resin: From natural waste to value-added biomaterial. *Thermochim. Acta* **2017**, *655*, 21–33. [CrossRef]

24. Liu, G.; Guomin, W.; Shuping, H.; Can, J.; Kong, Z. Synthesis and Properties of Non-Isoyanate Polyurethane Coatings derived from Cyclic Carbonate-Functionalized Polysiloxanes. *Prog. Org. Coat.* **2017**, *112*, 169–175. [CrossRef]

25. Xi, X.; Pizzi, A.; Gerardin, C.; Lei, H.; Chen, X.; Amirou, S. Preparation and evaluation of glucose based non-isocyanate polyurethane self-blowing rigid foams. *Polymers* **2019**, *11*, 1802. [CrossRef]

26. Xi, X.; Pizzi, A.; Gerardin, C.; Du, G. Glucose-biobased non-isocyanate polyurethane rigid foams. *J. Renew. Mater.* **2019**, *7*, 301–312. [CrossRef]

27. Chen, X.; Pizzi, A.; Fredon, E.; Gerardin, C.; Zhou, X.; Zhang, B.; Du, G. Low curing temperature tannin-based non-isocyanate polyurethane (NIPU) wood adhesives: Preparation and properties evaluation. *Int. J. Adhes. Adhes.* **2022**, *112*, 103001. [CrossRef]

28. Annunziata, L.; Diallo, A.K.; Fouquay, S.; Michaud, G.; Simon, F.; Brusson, J.-M.; Carpentier, J.-F.; Guillaume, S.M. α, ω-Di (*Glycerol carbonate*) telechelic polyesters and polyolefins as precursors to polyhydroxyurethanes: An isocyanate-free approach. *Green Chem.* **2014**, *16*, 1947–1956. [CrossRef]

29. Tundo, P.; Selva, M. The chemistry of dimethyl carbonate. *Acc. Chem. Res.* **2002**, *35*, 706–716. [CrossRef]

30. Xi, X.; Pizzi, A.; Delmotte, L. Isocyanate-free polyurethane coatings and adhesives from mono-and di-saccharides. *Polymers* **2018**, *10*, 402. [CrossRef]

31. Chen, X.; Pizzi, A.; Essawy, H.; Fredon, E.; Gerardin, C.; Guigo, N.; Sbirrazzuoli, N. Non-furanic humins-based non-isocyanate polyurethane (NIPU) thermoset wood adhesives. *Polymers* **2021**, *13*, 372. [CrossRef]

32. Thébault, M.; Pizzi, A.; Dumarçay, S.; Gerardin, P.; Fredon, E.; Delmotte, L. Polyurethanes from hydrolysable tannins obtained without using isocyanates. *Ind. Crops Prod.* **2014**, *59*, 329–336. [CrossRef]

33. Azadeh, E.; Chen, X.; Pizzi, A.; Gerardin, C.; Gerardin, P.; Essawy, H. Self-Blowing Non-Isocyanate Polyurethane Foams Based on Hydrolysable Tannins. *J. Renew. Mater.* **2022**, *10*, 3217–3227. [CrossRef]

34. Thébault, M.; Pizzi, A.; Essawy, H.A.; Baroum, A.; van Assche, G. Isocyanate free condensed tannin-based polyurethanes. *Eur. Polym. J.* **2015**, *67*, 513–526. [CrossRef]

35. Thébault, M.; Pizzi, A.; Santiago-Medina, F.J.; Al-Marzouki, F.M.; Abdalla, S. Isocyanate-free polyurethanes by coreaction of condensed tannins with aminated tannins. *J. Renew. Mater.* **2017**, *5*, 21–29. [CrossRef]

36. Tondi, G.; Pizzi, A. Tannin-based rigid foams: Characterization and modification. *Ind. Crops Prod.* **2009**, *29*, 356–363. [CrossRef]

37. Chen, M.J.; Chen, C.R.; Tan, Y.; Huang, J.-Q.; Wang, X.-L.; Chen, L.; Wang, Y.-Z. Inherently flame-retardant flexible polyurethane foam with low content of phosphorus-containing cross-linking agent. *Ind. Eng. Chem. Res.* **2014**, *53*, 1160–1171. [CrossRef]

38. Wang, S.X.; Zhao, H.B.; Rao, W.H.; Wang, T.; Liao, W.; Wang, Y.-Z. Inherently flame-retardant rigid polyurethane foams with excellent thermal insulation and mechanical properties. *Polymer* **2018**, *153*, 616–625. [CrossRef]

39. Dong, F.; Wang, Y.; Wang, S.; Shaghaleh, H.; Sun, P.; Huang, X.; Xu, X.; Wang, S.; Liu, H. Flame-retarded polyurethane foam conferred by a bio-based nitrogen phosphorus-containing flame retardant. *React. Funct. Polym.* **2021**, *168*, 105057. [CrossRef]

40. Zhang, M.; Luo, Z.; Zhang, J.; Chen, S.; Zhou, Y. Effects of a novel phosphorus–nitrogen flame retardant on rosin-based rigid polyurethane foams. *Polym. Degrad. Stab.* **2015**, *120*, 427–434. [CrossRef]

41. Li, J.; Zhang, A.; Zhang, S.; Gao, Q.; Zhang, W.; Li, J. Larch tannin-based rigid phenolic foam with high compressive strength, low friability, and low thermal conductivity reinforced by cork powder. *Compos. Part B Eng.* **2019**, *156*, 368–377. [CrossRef]

42. Xu, Y.; Han, Y.; Shi, S.Q.; Gao, Q.; Li, J. Preparation of a moderate viscosity, high performance and adequately-stabilized soy protein-based adhesive via recombination of protein molecules. *J. Clean. Prod.* **2020**, *255*, 120303. [CrossRef]

43. Chen, X.; Pizzi, A.; Xi, X.; Zhou, X.; Fredon, E.; Gerardin, C. Soy protein isolate non-isocyanates polyurethanes (NIPU) wood adhesives. *J. Renew. Mater.* **2021**, *9*, 1045–1057. [CrossRef]

44. Chen, X.; Xi, X.; Pizzi, A.; Fredon, E.; Zhou, X.; Li, J.; Gerardin, C.; Du, G. Preparation and characterization of condensed tannin non-isocyanate polyurethane (NIPU) rigid foams by ambient temperature blowing. *Polymers* **2020**, *12*, 750. [CrossRef]

45. Del Menezzi, C.; Amirou, S.; Pizzi, A.; Xi, X.; Delmotte, L. Reactions with Wood Carbohydrates and Lignin of Citric Acid as a Bond Promoter of Wood Veneer Panels. *Polymers* **2018**, *10*, 833. [CrossRef]